substance: $InAs_xSb_{1-x}$
property: physical properties

Only a few papers on this system have been published. OMVPE layers on Al_2O_3 have been grown [81N].

The band structure of $InAs_xSb_{1-x}$ has the pecularity that E_g passes through a minimum near x = 0.5.

For compositional dependence of energy gap, see Fig. 1, of electron effective mass, see Fig. 2.

energy gap bowing parameter

$c(\Gamma)$	0.672 eV	T = 10 K	photoluminescence, see also Fig. 12	90F

See also [69V, 67T, 69C]

temperature dependence of E_g: see [98M]

electron mobility

see Fig. 13

hole mobility
(for x = 0.91)

$\mu_{H,p}$	70 cm^2/Vs	T = 290 K	Hall effect	95K
	141 cm^2/Vs	T = 77 K		

Further properties

Miscibility gap [89I].
Enthalpies of mixing [95R]
Thermochemical data and assessed phase diagram [98L].

Further figures and references:

Figs. 3...11, [67T, 68C, 68T, 71T, 72V, 68A, 70L]

References:

64W Woolley, C. J., Warner, J.: Can. J. Phys. 42 (1964) 1879.
67T Thompson, A. U., Woolley, J. C.: Can. J. Phys. 45 (1967) 255.
68A Aubin, M. J., Woolley, J. C.: Can. J. Phys. 26 (1968) 1191.
68C Coderre, W. M., Woolley, J. C.: Can. J. Phys. 46 (1968) 1207.
68T van Tongerbo, F. H.,Woolley, J. C.: Can. J. Phys. 46 (1968) 1199.
69C Coderre, W. M., Woolley, J. C.: Can. J. Phys. 48 (1969) 463.
69V Vishnubhatla, S. S., Eyglunent, B., Woolley, J. C.: Can. J. Phys. 47 (1969) 1661.
70L Lucovski, G., Chen, M. F.: Solid State Commun. 8 (1970) 1397.
71T Thomas, M. B., Woolley, J. C.: Can. J. Phys. 49 (1971) 2052.
72P Panish, M. B., Ilegems, M.: Progress in Solid State Chemistry, H. Reiss, JO. McCaldin eds., Pergamon Press, New York 1972, p. 39.
72S Stringfellow, G. B.: J. Phys. Chem. Solids 33 (1972) 665.
72V van Vechten, J. A., Berolo, O., Woolley, J. C.: Phys. Rev. Lett. 29 (1972) 1400.
81N Nataf, G., Verie, C.: J. Cryst. Growth 55 (1981) 87.
82B Burkhard, H., Dinges, H. W., Kuphal, E.: J. App]. Phys. 53 (1982) 655.
88Y Yen, M. Y., People, R., Wecht, K. W., Cho, A. Y.: Appl. Phys. Lett. 52 (1988) 489.
89I Ishida, K., Nomura, T., Tokunaga, H., Ohtani, H., Nishizawa, T.: J. Less-Common Met. 155 (1989) 193.
90F Fang, Z. M., Ma, K. Y., Jaw, D. H., Cohen, R. M., Stringfellow, G. B.: J. Appl. Phys. 67 (1990) 7034.
95K Krier, A., Mao, Y.: Semicond. Sci. Technol. 10 (1995) 930.
95R Rugg, B.C., Silk, N.J., Bryant, A.W., Argent, B.O.: CALPHAD: Comput. Coupling Phase Diagrams Thermochem. 19 (1995) 389.
98L Li, J.-B., Zhang, W., Li, Ch., Du, Zh.: J. Phase Equilibria 19 (1998) 473.
98M Marciniak, M. A., Hengehold, R. L., Yeo, Y. K., Turner, G. W.:J. Appl. Phys. 84 (1998) 480.

Fig. 1.

$InSb_{1-x}As_x$. Compositional dependence of the extrapolated absolute-zero band gap. Open circles from Hall effect measurements, full circles: extrapolated values from optical measurements [68C].

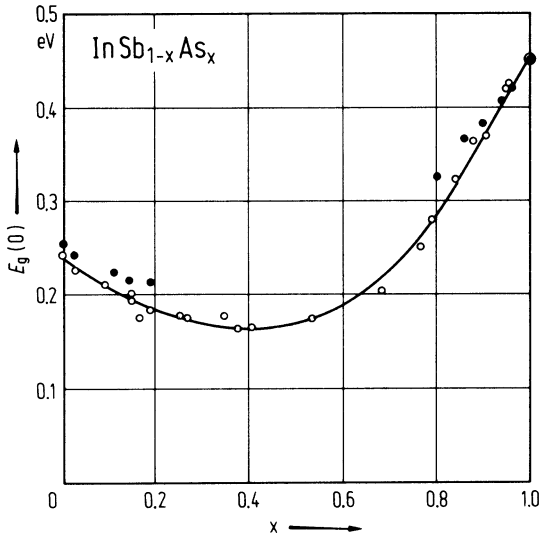

Fig. 2.

$InSb_{1-x}As_x$. Compositional dependence of the electron effective mass. Full circles: plasma reflectance, open circles: Faraday rotation, triangles: magnetothermoelectric power [71T].

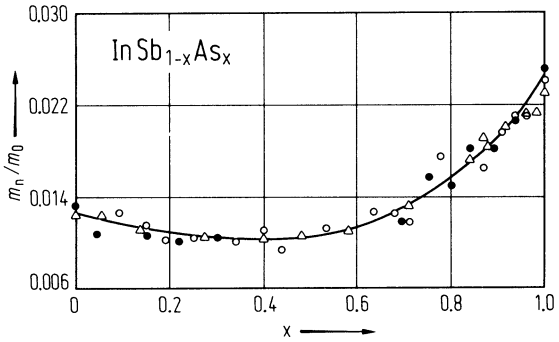

Fig. 3.

$InAs_xSb_{1-x}$. Composition dependence of the optical energy gap at room temperature. Open circles: transmission, full circles: photoconductivity, triangles and bars: diffuse reflectivity measurements [64W].

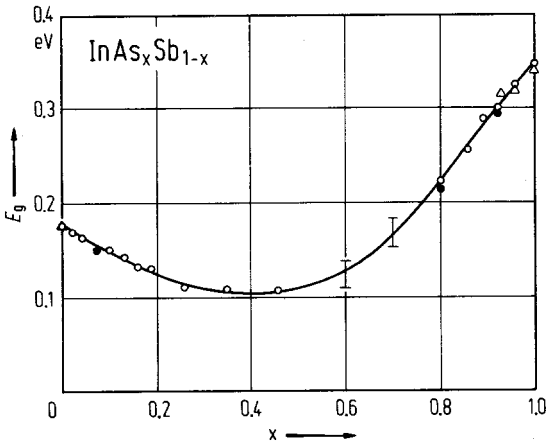

Fig. 4.

$InAs_xSb_{1-x}$. Composition dependence of higher energy electroreflectance peaks [69V].

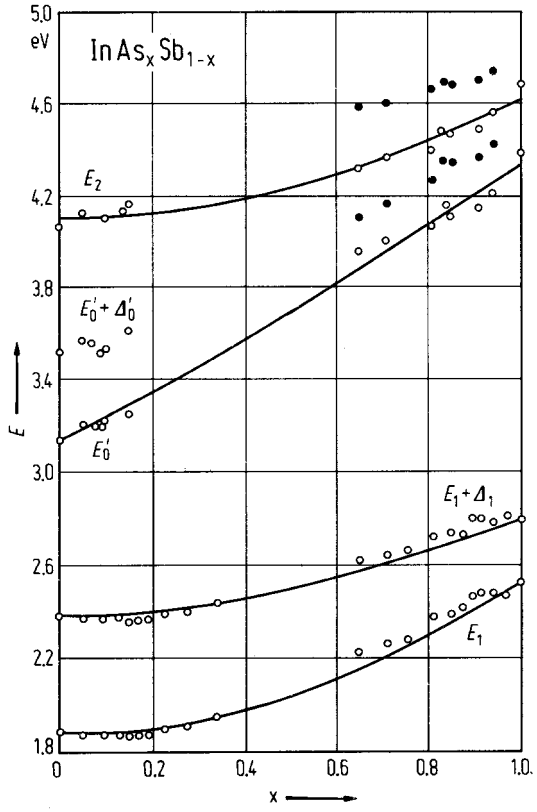

Fig. 5.

$InAs_xSb_{1-x}$. Composition dependence of spin-orbit splitting energies $\Delta_0$and $\Delta_1$and theoretical curves [72V].

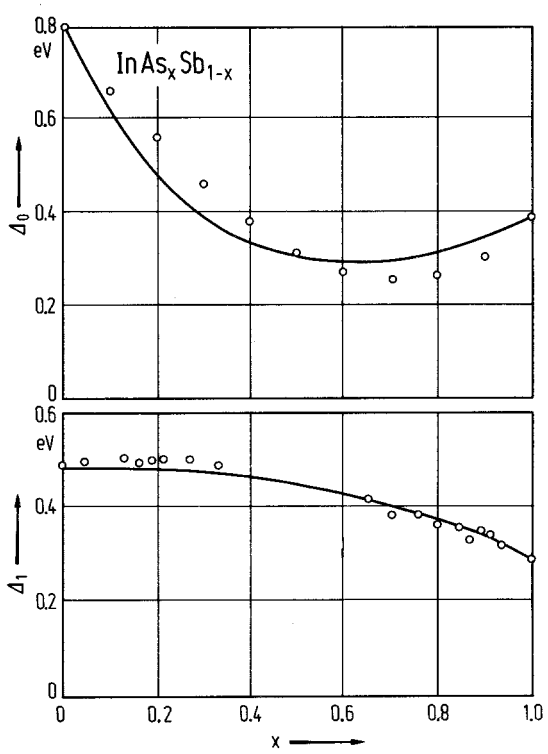

Fig. 6.

$InAs_xSb_{1-x}$. Composition dependence of the electron mobility at various temperatures for samples with about 10^{17} carriers/cm^3 [68C]. Solid lines: linear interpolation.

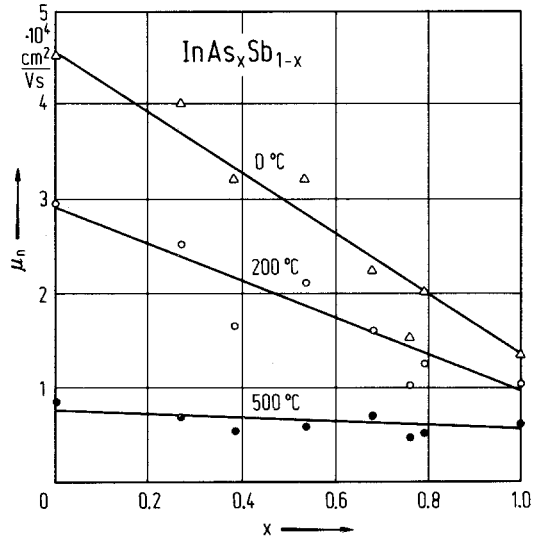

Fig. 7.

$InAs_xSb_{1-x}$. Composition dependence of the parameter Θ of the temperature dependence of the electron mobility $\mu_n = \mu_0 \exp(-T/\Theta)$ [68C].

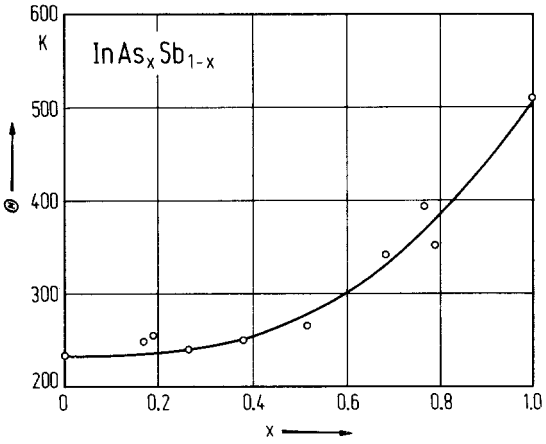

Fig. 8.

$InAs_xSb_{1-x}$. Variation of the dielectric constant with the square of the wavelength for x = 0.05 (curve *1*), 0.22 (*2*), 0.30 (*3*) and 0.84 (*4*) [71T].

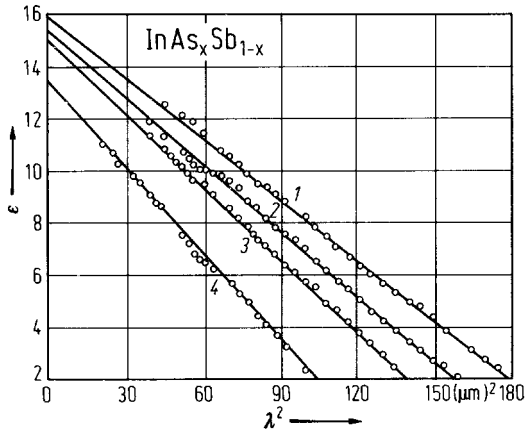

Fig. 9.

$InAs_xSb_{1-x}$. Liquidus isotherms in the In–InSb–InAs part of the ternary In–As–Sb system [72P]. Solid lines calculated.

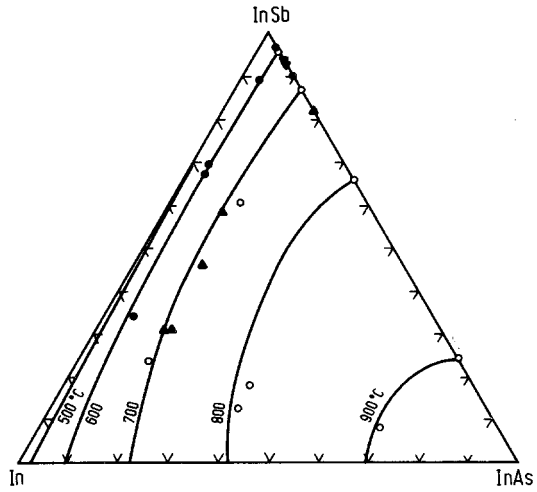

Fig. 10.

$InAs_xSb_{1-x}$. Pseudobinary phase diagram [72S]. Solid lines calculated.

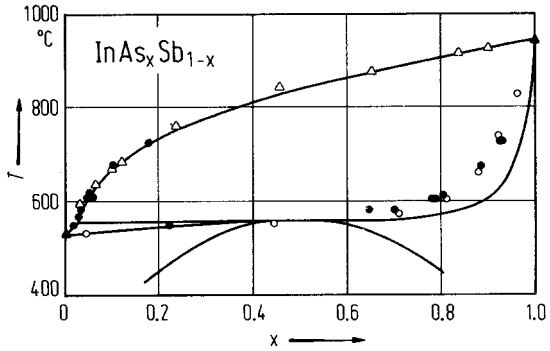

Fig. 11.

III–V solid solutions. Variation of lattice parameter in various pseudobinary systems. Immiscibility is indicated by broken lines [64M].

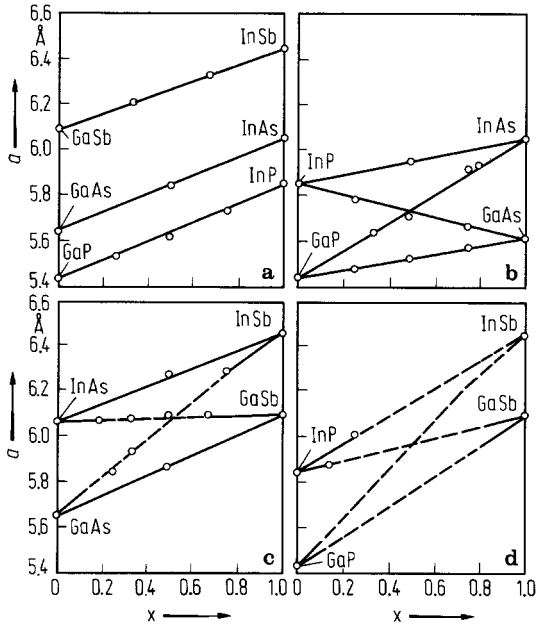

Fig. 12.

$InAs_{1-x}Sb_x$. Low-temperature (10 K) photoluminescence peak energies vs. composition [90F] (full circles). The solid curve is a least square fit to the closed circles. Earlier results are from [68C] (open triangles) and from [88Y] (crosses).

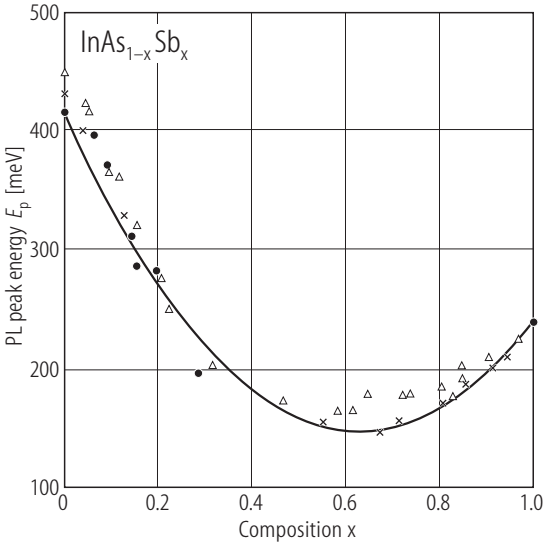

Fig. 13.

$InAs_{1-x}Sb_x$. Room-temperature electron mobility as a function of alloy composition [95K]. Star: sample grown on GaSb by LPE; squares and full circles : samples grown by MBE on GaAs and InP.